

The Low- $\delta^{18}\text{O}$ Late-Stage Ferrodiorite Magmas in the Skaergaard Intrusion: Result of Liquid Immiscibility, Thermal Metamorphism, or Meteoric Water Incorporation into Magma?

I. N. Bindeman, C. K. Brooks,¹ A. R. McBirney, and H. P. Taylor²

Department of Geological Sciences, 1272 University of Oregon, Eugene, Oregon 97403, U.S.A.
(e-mail: bindeman@uoregon.edu)

ABSTRACT

We report new laser fluorination oxygen isotope analyses of selected samples throughout the Skaergaard intrusion in East Greenland, particularly relying on ~ 1 -mg separates of the refractory, alteration-resistant minerals zircon, sphene, olivine, and ferroamphibole. We also reexamine published oxygen isotope data on bulk mineral separates of plagioclase and clinopyroxene. Our results show that the latest-stage, strongly differentiated magmas represented by ~ 3 to 6 km^3 of ferrodiorites around the Sandwich Horizon (SH), where the upper and lower solidification fronts met, became depleted in ^{18}O by about 1.5‰–2‰ relative to the original Skaergaard magma and the normal mantle-derived mid-ocean ridge basalt. Earlier studies did not recognize these low- $\delta^{18}\text{O}$ ferrodiorite magmas ($\delta^{18}\text{O} = \sim 3\text{‰}–4\text{‰}$) because after the intrusion solidified, much of the intrusion and its overlying roof rocks were heavily overprinted by low- $\delta^{18}\text{O}$ meteoric-hydrothermal fluids. We consider three possible ways of producing these low- $\delta^{18}\text{O}$ ferrodiorite magmas. (1) At isotopic equilibrium, liquid immiscibility may cause separation of a higher- $\delta^{18}\text{O}$, higher- SiO_2 granophyric melt, thereby depleting the residual Fe-rich ferrodiorite magma in ^{18}O . However, such a model would require removal of many cubic kilometers of coeval granophyre, a greater proportion than is observed anywhere in the intrusion; there is no evidence that any such magmas erupted to the surface and were eroded. (2) While direct migration of low- $\delta^{18}\text{O}$ water seems implausible, we consider a model of “self-fertilization,” whereby oxygen from meteoric waters entered the SH magma by devolatilization and exchange with hydrated, low- $\delta^{18}\text{O}$ stopped blocks of the upper border series. Such reactive exchange between residual melt and adjacent hydrothermally altered, water-saturated rocks contributed low- $\delta^{18}\text{O}$ crystalline components and low- $\delta^{18}\text{O}$ pore water to the residual melt. The low- $\delta^{18}\text{O}$ zircon and sphene may have crystallized directly from this contaminated low- $\delta^{18}\text{O}$ melt, even though the entire mineral assemblage did not, simplifying the mass balance problem. (3) Finally, after SH crystallization, fracturing, and subsequent subsolidus meteoric-hydrothermal alteration depleted these rocks in ^{18}O , intrusion of the 660-m-thick Basistoppen sill, emplaced 150–200 m above the still hot SH, may have reheated and partially melted these late-stage differentiates. In this scenario, zircon and sphene could have crystallized from a low- $\delta^{18}\text{O}$ partial melt, while other minerals may have simply reequilibrated. We favor models 2 and 3 and discuss their strengths and weaknesses.

Online enhancements: appendix, figure.

Introduction

The Tertiary Skaergaard intrusion in East Greenland has, for more than 70 yr, been a classic locality not only for the study of layered igneous complexes but also for understanding magmatic differentiation in general (Wager and Deer 1939; Wager and Brown 1967; Brooks 1969; Brooks et al. 1991; McBirney

1995, 1996; Nielsen 2004). A chamber measuring $\sim 300 \text{ km}^3$ (fig. 1) was filled by essentially one pulse of tholeiitic magma and differentiated in place with minimum contamination from the country rocks to form unusually iron-rich ferrodiorites and subordinate amounts of granophyre (typically as pods and segregation veins). However, the precise nature of the liquid line of descent is still in dispute (Hunter and Sparks 1987; Brooks and Nielsen 1990; McBirney and Naslund 1990; Morse 1990), as is the precise mechanism of differentiation (McBirney and Noyes 1979; Irvine et al. 1998). The Skaergaard

Manuscript received February 7, 2008; accepted July 15, 2008.

¹ Institute of Geology, University of Copenhagen, Østervoldgade 10, 1350 Copenhagen, Denmark.

² Geological and Planetary Sciences, California Institute of Technology, Pasadena, California 91125, U.S.A.

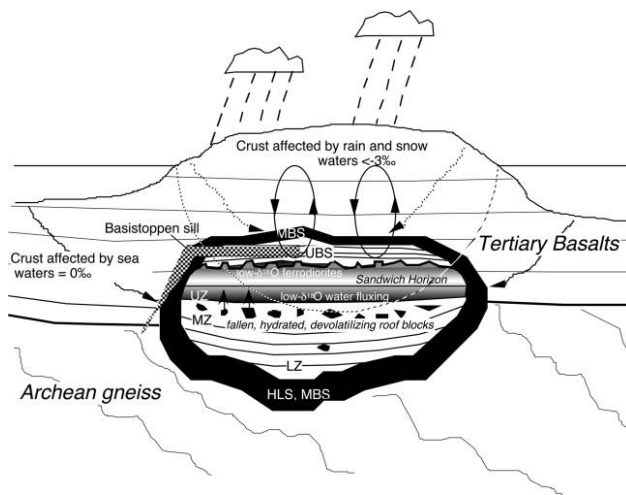


Figure 1. Schematic cross section through the Skaergaard intrusion, showing the principal stratigraphic units, Sandwich Horizon, Basistoppen sill, fallen blocks, and Tertiary paleotopography, based on data that indicate shallow emplacement (1.5–3 km below the surface; McBirney 1996; Larsen and Tegner 2006) and the possible existence of an island above the intrusion.

intrusion has recently attracted new scientific and commercial interest with the discovery of a major palladium-gold zone (Brooks et al. 1999; Nielsen et al. 2005).

The initial study of Skaergaard by Taylor and Epstein (1963) was for the purpose of determining the primary oxygen and hydrogen isotopic changes that occur in igneous rocks during differentiation. Their results, however, showed that the dominant isotopic changes in Skaergaard were, in fact, the result of pervasive alteration by meteoric-hydrothermal fluids (Taylor 1968). Taylor and Forester (1979) used conventional laboratory techniques to make a detailed oxygen and hydrogen isotope study of the intrusion, its country rocks, and the xenoliths and stoped blocks. They showed that the intrusion drove an extensive shallow meteoric-hydrothermal system that affected the rate of cooling and crystallization of the intrusion. Many gabbros that appear perfectly fresh and mineralogically unaltered in thin section can be shown to have exchanged oxygen isotopes with these low- $\delta^{18}\text{O}$ meteoric waters, commonly at temperatures of 400°–600°C. Norton and Taylor (1979) modeled this hydrothermal system and obtained a good match between the computer calculations and the measured variations of $\delta^{18}\text{O}$ in alteration-susceptible plagioclase throughout the intrusion. Using this model, they were able to estimate water/

rock ratios as a monitor of the intensity of hydrothermal circulation throughout the intrusion.

Taylor and Forester (1979, p. 393) suggested that the Skaergaard intrusion was initially mid-ocean ridge basalt (MORB)-like in terms of its major elements, including oxygen. The tremendous ranges in $\delta^{18}\text{O}$ values of whole rocks and minerals were interpreted to be caused entirely by postcrystallization hydrothermal circulation driven by the cooling intrusion itself. They also noted, however, that the uppermost part of the layered series (UZc) and the lowermost part of the upper border series (UBS γ) both exhibited consistently lower clinopyroxene $\delta^{18}\text{O}$ values, relative to coexisting plagioclase, than did the rocks that crystallized earlier at either the top or the bottom of the intrusion (fig. 1). This difference was attributed to subsolidus inversion of the primary precursor mafic mineral (ferrobustamite) in these latest-crystallizing parts of the intrusion. These crystals inverted on cooling to a very fine-grained mosaic of hedenbergitic clinopyroxenes, and this was presumed to have made them more susceptible than the normal-sized clinopyroxene grains to secondary exchange with meteoric waters. Nevertheless, Taylor and Forester (1979) were not able to rule out the possibility that these consistently lower clinopyroxene $\delta^{18}\text{O}$ values in UZc and UBS γ might instead be a primary low- $\delta^{18}\text{O}$ magma signature.

Answering the question of whether Skaergaard was indeed a low- $\delta^{18}\text{O}$ magma at any stage during its evolution (i.e., that it may have contained oxygen derived from meteoric waters while still in the molten state) is important because it will require modifications to the earlier models in the literature describing Skaergaard as an archetypical example of closed-system crystallization differentiation. It may also have relevance for explaining siliceous felsic rocks in this part of the intrusion as products of closed-system differentiation, liquid immiscibility, or partial melting of stoped blocks. Moreover, the origin of the Pd-Au mineralization may have been dependent on the nature, timing, and role of hydrothermal fluids.

Here we present laser fluorination analyses (table 1) of the refractory accessory minerals zircon and sphene, which should have been relatively immune to the subsequent hydrothermal alteration (e.g., Valley et al. 2003). We also report oxygen isotopic analyses of individual and bulk crystals olivine, clinopyroxene, amphibole, and quartz that rely only on ~1 mg of the best, least altered material. These data might allow us to see through some of the secondary effects documented by

Table 1. Oxygen Isotopes in Selected Samples from Skaergaard Intrusion (East Greenland) by Laser Fluorination Analyses

Sample and mineral	$\delta^{18}\text{O}$ (‰ VSMOW)
Coeval basalts:	
KB-04:	
Olivine	5.25
Olivine	5.30
Olivine	5.53
Picrite, Miki fiord:	
Olivine	4.90
Skaergaard:	
Marginal border group:	
SK-656, few meters from lower contact on east side of intrusion:	
Plag	5.37
Cpx-1, black	4.99
Olivine	4.55
Olivine	5.25
Sphene	4.54
Lower border series:	
SK-218, pegmatite (Larsen and Brooks 1994):	
Quartz	7.27
Plag	5.76
Amphibole	2.96
Zircon, bulk	4.44
Zircon, bulk	4.33
Zircon, >151 μm	4.24
Zircon, <53 μm	3.78
Middle zone:	
SK-103, pegmatite: ^a	
Quartz	6.08
Plag	5.60
Amphibole	3.85
Cpx	4.36
Sandwich Horizon (SH), geochronology sample, 55.59 Ma:	
428-1:	
Plag	5.49
Zircon, bulk	3.26
Zircon, bulk	3.25
Sphene	3.03
Sphene	2.95
Sphene	3.00
Amphibole	3.03
Upper zone c (UZc):	
SK-332, few meters below SH, 25 wt% FeO, with inverted Cpx:	
Plag	5.50
Cpx-1, green	2.03 (inverted)
Cpx, bulk green	1.86 (inverted)
Cpx, black	4.15 (uninverted)
SK-333, few meters below SH, 25 wt% FeO, with uninverted Cpx:	
Cpx, two crystals	4.05
Cpx-1, black	3.97
Cpx-1 black	4.42
SK-15, UZc, with uninverted Cpx:	
Plag	5.16
Olivine	3.64
Olivine	3.41
Cpx-1, black	4.26
SK-334, ^a UZc pegmatite, few meters below SH, with inverted Cpx:	
Plag	5.24
Sphene	3.74
Sphene	3.91
Cpx-1, green	2.06 (inverted)

(Continued)

Table 1. (Continued)

Sample and mineral	$\delta^{18}\text{O}$ (‰ VSMOW)
Upper border series γ :	
SK-335, few meters above SH, with inverted Cpx:	
Plag	5.05
Cpx	2.60 (inverted)
KG-423, 30 m above SH, with inverted Cpx, hydrothermally altered Zr-rich sample near Brooks Horizon:	
Plag	2.25
Cpx-1	-0.19
Cpx-1	-0.44
Zircon, bulk	2.00
Zircon, bulk	1.96
SK-336, ^a 100 m above SH, with uninverted Cpx, fresh plag:	
Plag	4.03
Cpx-1	2.45
Basistoppen intrusion:	
SK-76, uninverted Cpx, hydrothermally altered plag:	
Cpx-1, brown	5.34
Cpx-1, brown	4.92
Sydtoppen intrusion, granophyre on top of Basistoppen:	
SK-88:	
Qz-1	5.88
Plag-1	4.42
Zircon, >151 μm	4.50

Note. Cpx-1 = single crystal analysis.

^a Zircon extraction yielded no or insignificant amounts of zircon.

Taylor and Forester (1979), who analyzed only conventional mineral separates 20–30 mg in size.

Results

Primary Magma. Figure 2 presents the crystallization stratigraphy of Skaergaard and plots $\delta^{18}\text{O}$ values of major and accessory minerals analyzed in this work, comparing them with analyses of clinopyroxene from Taylor and Forester (1979). To help constrain the $\delta^{18}\text{O}$ value of primary magma, we also analyzed minerals in certain rocks that were coeval with the intrusion (e.g., Larsen et al. 1989; Larsen and Tegner 2006). (i) Analyses of olivine crystals in lavas that were contemporary with or earlier than the intrusion demonstrate that they are mantlelike at $5.25\text{‰} \pm 0.2\text{‰}$, thus suggesting MORB-like $\delta^{18}\text{O}$ values for the contemporaneous mantle plume. (ii) The earliest crystallized Skaergaard rocks are those in chilled margins and the hidden layered series (HZ; figs. 1, 2). The latter consist of picritic gabbros and troctolites and are thought to represent only about 10% of the intrusion's original volume (Blank and Gettings 1973). The coexisting minerals in the eastern marginal border series (MBS; sample SK-656) record somewhat lower but mantlelike $\delta^{18}\text{O}$ values (fig. 2), similar to those in contemporaneous basalts. (iii) A late but coeval gabbroic

intrusion into the Skaergaard UBS (Basistoppen sill, sample SK-76) also records mantlelike $\delta^{18}\text{O}_{\text{Cpx}}$ values. These data firmly constrain the boundary conditions and initial composition for Skaergaard as normal, mantlelike $\delta^{18}\text{O}$.

Main Volume Skaergaard and the Effects of Plutonic Cooling. If we consider only those Skaergaard samples from Taylor and Forester (1979) in which plagioclase records little or no hydrothermal alteration (based on the criteria of preserving $\delta^{18}\text{O}_{\text{plag}} = 5.7\text{--}6.4$ and $\Delta^{18}\text{O}[\text{plag} - \text{cpx}] = 0.8\text{‰}\text{--}1.3\text{‰}$), we obtain uniform $\delta^{18}\text{O}_{\text{Cpx}}$ values of $4.98\text{‰} \pm 0.15\text{‰}$ ($n = 11$); these sample localities are scattered across the intrusion in the lower zone (LZ), middle zone (MZ), bottommost upper zone (UZa), middlemost upper zone (UZb), and MBS. As shown in figure 3, such $0.8\text{‰}\text{--}1.3\text{‰} \Delta^{18}\text{O}[\text{plag} - \text{cpx}]$ values represent equilibrium at high temperature ($\sim 750\text{--}950\text{°C}$ for $\text{An}_{70-40}\text{-Cpx}$; e.g., Chiba et al. 1989). However, these $4.98\text{‰} \pm 0.15\text{‰} \delta^{18}\text{O}_{\text{Cpx}}$ values are lower than the presumed values of the original liquidus Skaergaard pyroxenes, which probably formed at $\sim 1100\text{°C}$ with a characteristic mantle clinopyroxene value of about 5.4‰ , in equilibrium with mantle olivine at $5.2\text{‰} \pm 0.2\text{‰}$ (e.g., Anderson et al. 1971; Eiler 2001) and mantle zircon at $5.3\text{‰} \pm 0.3\text{‰}$ (Valley 2003). We attribute the $0.2\text{‰}\text{--}0.6\text{‰}$ lowering of

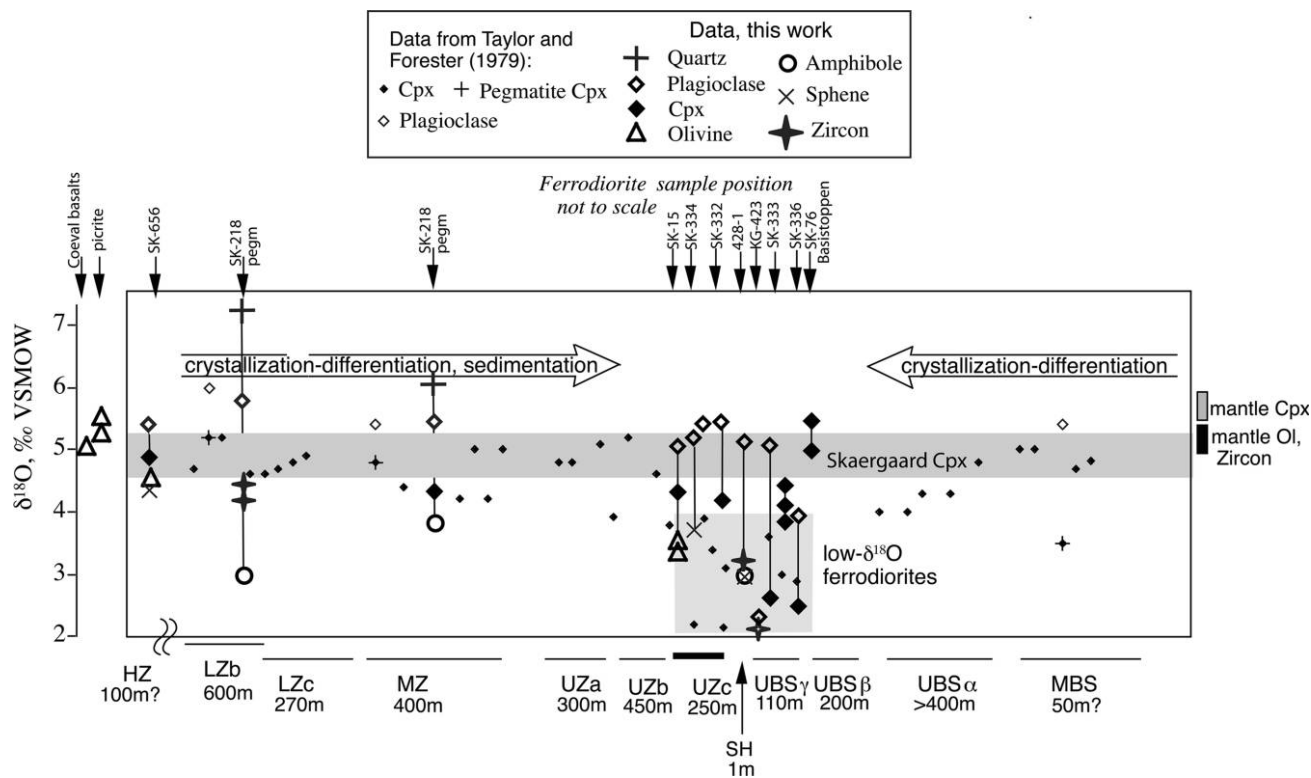


Figure 2. The $\delta^{18}\text{O}$ values of minerals analyzed in this study plotted schematically (i.e., not to scale) against their stratigraphic position from bottom (*left*) to top (*right*) in the Skaergaard intrusion. See table 1 for individual analyses. Stratigraphic nomenclature and thicknesses are from Wager and Brown (1967). Also included on the diagram are the clinopyroxene data from table 10 of Taylor and Forester (1979). Skaergaard crystallization proceeded from both the floor and the roof, culminating in the low- $\delta^{18}\text{O}$ ferrodiorites (SK-15 to SK-333) surrounding the Sandwich Horizon.

$\delta^{18}\text{O}_{\text{Cpx}}$ values to the effects of plutonic cooling that promoted closed-system isotopic exchange among clinopyroxene, plagioclase, and interstitial melt, thereby recording lower temperatures and larger $\Delta^{18}\text{O}$ values (fig. 3). Furthermore, closed-system inward crystallization of the intrusion is also accompanied by increasingly Na-rich plagioclase, leading to greater $\Delta^{18}\text{O}[\text{plag} - \text{cpx}]$ values (O'Neil and Taylor 1967; Chiba et al. 1989). As shown in figure 3, the net result is that for evolved Skaergaard rocks, it is expected that at equilibrium, $\delta^{18}\text{O}_{\text{Oplag}}$ should increase while $\delta^{18}\text{O}_{\text{Cpx}}$ values should decrease on cooling (and with decreasing anorthite content of plagioclase).

Excluding the 11 unaltered samples, all of the other Skaergaard clinopyroxenes analyzed by Taylor and Forester (1979) have lower $\delta^{18}\text{O}_{\text{Cpx}}$ values of 0.7‰–4.9‰, and many of them coexist with very ^{18}O -depleted plagioclase. Together with their coexisting feldspars, these other samples record a huge range of $\Delta^{18}\text{O}[\text{plag} - \text{cpx}]$ values, from -5.0% to $+1.9\%$. Their $\delta^{18}\text{O}_{\text{Oplag}}$ values

range from 1.4‰ to 5.5‰; thus, the meteoric-hydrothermal fluids that drastically lowered the $\delta^{18}\text{O}_{\text{Oplag}}$ values also had some effect on the coexisting pyroxenes. We therefore do not interpret the somewhat ^{18}O -depleted clinopyroxenes shown in figure 2 as indicating that the external low- $\delta^{18}\text{O}$ oxygen reservoir had any measurable effect on the bulk of the Skaergaard magma body before its crystallization.

The latest stages of Skaergaard solidification (UZc, UBS γ) in the upper part of the intrusion present a different story. The minerals in these ferrodiorites are all characterized by very low $\delta^{18}\text{O}$ values, and these are also the most evolved, high-Fe/Mg, high-Na/Ca differentiates found at Skaergaard; they surround the Sandwich Horizon (SH), where the upper and lower solidification fronts met (fig. 1). In addition, this is the part of the intrusion where we observe anomalous plagioclase-clinopyroxene $\delta^{18}\text{O}$ relationships, such that one cannot a priori rule out the possibility that these minerals crystallized from a low- $\delta^{18}\text{O}$ magma

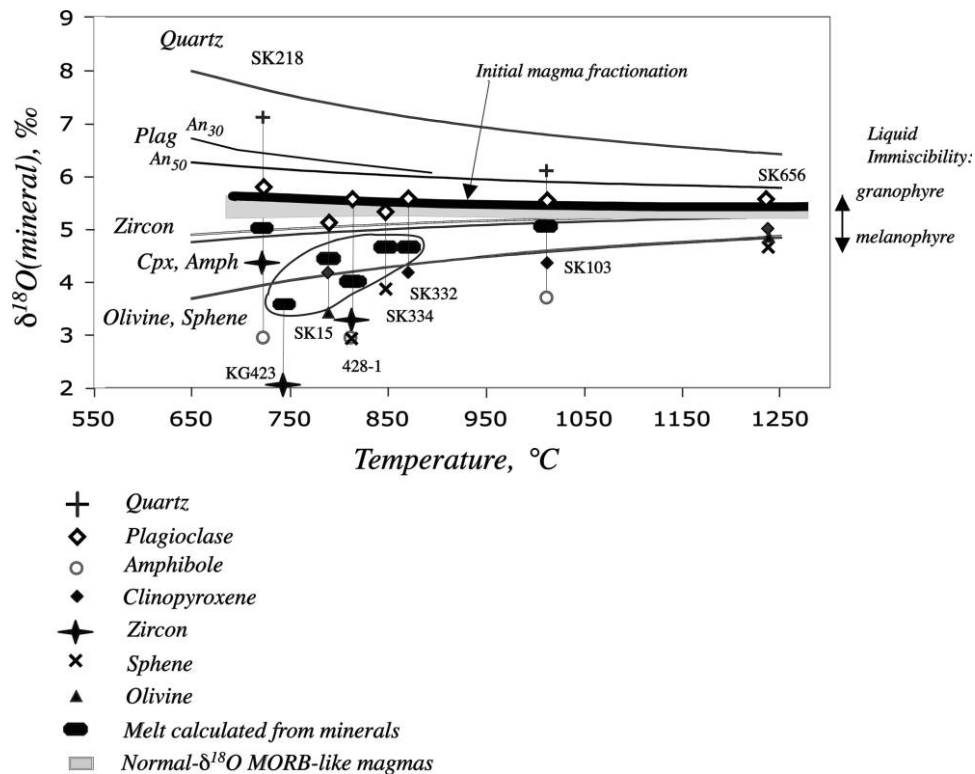


Figure 3. Equilibrium oxygen isotope fractionations as a function of temperature. Mineral-mineral isotope fractionation factors are from Chiba et al. (1989). Notice that fractionation factors and isotopic differences between minerals increase with decreasing temperatures and increasing degree of differentiation, with plagioclase and quartz $\delta^{18}\text{O}$ values increasing while accessory mineral, olivine, and clinopyroxene $\delta^{18}\text{O}$ values are decreasing. The rectangular box indicates the initial $5.5\% \pm 0.2\%$ Skaergaard magma $\delta^{18}\text{O}$ value. The $\delta^{18}\text{O}$ mineral values for samples of ferrodiorites and the initial chilled-margin gabbro (SK-656) are plotted at their most plausible crystallization temperatures. Note that the calculated $\delta^{18}\text{O}$ magma values for differentiated ferrodiorites plot below those of the initial Skaergaard magma and the estimated Skaergaard magma differentiation trend (*black band*; this closed-system trend from high to low temperatures was calculated using Bindeman et al.'s [2004] approach, which takes into account temperatures and mineral-mineral isotope fractionation factors and treats melt as a mixture of CIPW normative minerals). Isotope effects of liquid immiscibility of a hypothetical upper zone magma partitioned into a higher- $\delta^{18}\text{O}$ granophyre and lower- $\delta^{18}\text{O}$ melanophyre are shown on the right.

(see Taylor and Forester 1979, pp. 391–393). Unfortunately, most clinopyroxenes in these rocks are represented by crystals of inverted hedenbergite that consist of many 10–50- μm domains with random extinction under the microscope. Our laser fluorination analyses of single, inverted $\sim 1\text{-mg}$ clinopyroxene crystals around the SH yielded $\delta^{18}\text{O}$ values that plot in a 4.2‰–2.4‰ range, comparable to 20–30-mg bulk clinopyroxene analyses by Taylor and Forester (1979). Laser fluorination analysis of single, uninverted clinopyroxene and freshest plagioclase crystals in unaltered samples yielded values of $4.2\% \pm 0.2\%$ and $5.2\% \pm 0.2\%$, respectively; this is $\sim 1\%$ lower than the expected $\delta^{18}\text{O}_{\text{Cpx}}$ and $\delta^{18}\text{O}_{\text{plag}}$ values for Na-rich plagioclase at $\sim 750^\circ\text{C}$ (fig. 3). In order to resolve whether the

low- $\delta^{18}\text{O}_{\text{Cpx}}$ values are primary magmatic or secondary hydrothermal, we attempted to characterize these rocks further by analyzing their refractory accessory minerals zircon, sphene (table 1), olivine, and amphibole.

Low- $\delta^{18}\text{O}$, Late-Stage Differentiated Magmas Constrained by Refractory Minerals. The critical new evidence showing that the late-stage ferrodiorites in the vicinity of the SH crystallized from a low- $\delta^{18}\text{O}$ magma comes from the refractory minerals zircon, sphene, and fresh ferroamphibole (fig. 4). This conclusion is also supported by new analyses of noninverted clinopyroxenes from rocks collected within a few tens of meters of the SH, as shown in figure 2. These minerals, especially zircon, are known to be very resistant to the type of secondary

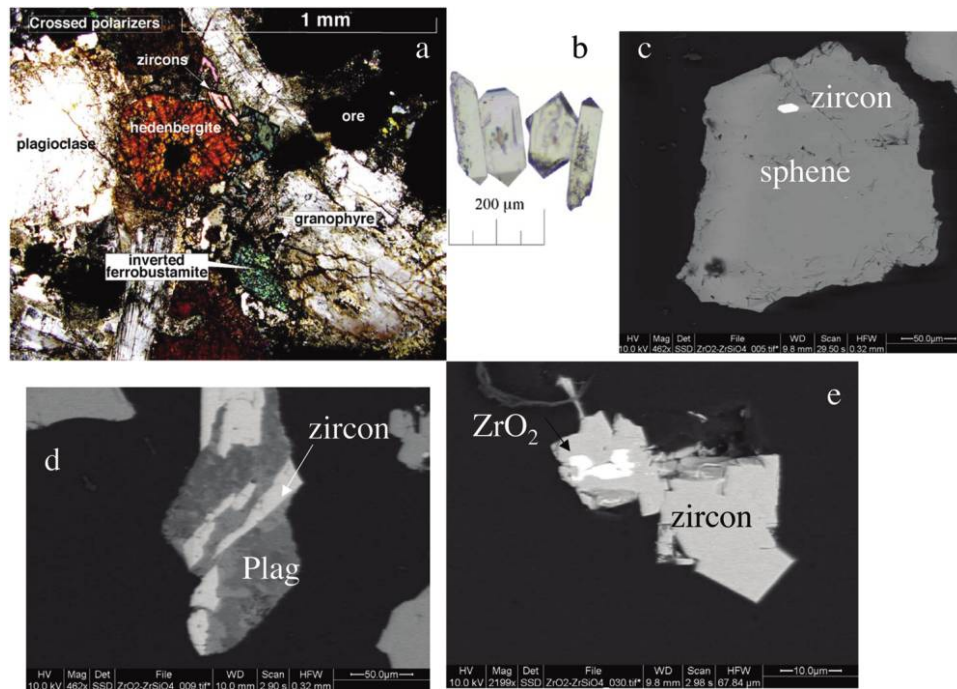


Figure 4. Photomicrographs (*a, b*) and backscattered electron imaging (*c–e*) of minerals from the Sandwich Horizon; *a* and *b* are from a sample equivalent to 428-1 (table 1).

meteoric-hydrothermal alteration that strongly affected the plagioclase (and perhaps the inverted clinopyroxenes) throughout much of the intrusion. Zircon and sphene from the SH (sample 428-1; table 1) have $\delta^{18}\text{O} = 3.25\%$ and 3.0% , respectively, at least 1.5% lower than their normal mantle values; they also display small (i.e., near-magmatic) isotope fractionations with coexisting minerals. Sample KG-423, collected 30 m above the SH, has $\delta^{18}\text{O}[\text{zircon}]$ values of 2.0% , 3% lower than the values for mantle. In this sample, clinopyroxene is inverted, and the hydrothermally altered plagioclase has low $\delta^{18}\text{O} = 2.25\%$, markedly out of equilibrium with the zircon. This sample is located in $\text{UBS}\gamma$ in the vicinity of the so-called Brooks Horizon, which is the most incompatible-element-rich portion of the Skaergaard intrusion (Brooks 1969; McBirney 2002), some 40 m below the base of the Basistoppen sill (fig. 1).

We failed to extract zircon from any of the other rocks around the SH by either conventional or hydrofluoric-acid-solution methods. Sphene in pegmatitic sample SK-334, below the SH, appears to be fresh and has $\delta^{18}\text{O} = 3.8\%$. Analyses of fresh olivine in sample SK-15 yielded values of 3.4% – 3.6% , 1.5% lower than those for mantle. This sample, collected near the eastern extremity of UZc and a few meters below the SH, is one of a very few

UZc samples that contain uninverted clinopyroxenes; the low $\delta^{18}\text{O}_{\text{Opx}}$ value of 4.26% in this sample, in high-temperature equilibrium with fresh coexisting plagioclase (5.16%), strongly suggests that the entire assemblage olivine-plagioclase-clinopyroxene crystallized from a low- $\delta^{18}\text{O}$ magma. Using the new data in figure 2, we calculate a $\delta^{18}\text{O}$ value of about 3% – 4% for the magma that formed the SH and adjacent ferrodiorites.

We conclude that the lens-shaped sheet of ferrodioritic magma centered around the SH in the upper part of the Skaergaard intrusion somehow became depleted in ^{18}O by at least 1.5% but locally perhaps by as much as 3% , relative to the initial Skaergaard magma. Given that two samples containing low- $\delta^{18}\text{O}$ zircons define a $\sim 30\text{-m}$ -thick layer, the zone of low- $\delta^{18}\text{O}$ magmas may extend from slightly below the SH through the lower third of $\text{UBS}\gamma$. Without more detailed sampling, it will be difficult to estimate the true vertical extent of the rocks that crystallized from low- $\delta^{18}\text{O}$ magmas; this could be as little as 30 m around the SH, as our new isotopic evidence requires, to as much as 200–300 m through the entire thickness of UZc and much of $\text{UBS}\gamma$ (fig. 2), i.e., in ferrodiorites that are compositionally closely analogous (Nielsen 2004) to the low- $\delta^{18}\text{O}$ SH. The latter interpretation is supported by the newly analyzed sample SK-336, collected

100 m above the SH and containing uninverted clinopyroxene, with $\delta^{18}\text{O} = 2.4\text{‰}$, that seemingly preserves high- T magmatic fractionation with coexisting plagioclase ($\delta^{18}\text{O} = 4.03\text{‰}$; table 1). Unfortunately, no refractory minerals were available to be analyzed from this sample. In any case, even including SK-336, the low- $\delta^{18}\text{O}$ magmas would constitute <5 vol% of the intrusion.

Hamilton and Brooks (2004) report zircon ages from SH sample 428-1 as being 55.59 ± 0.13 Ma, within error identical to the Ar-Ar age of the intrusion, 55.48 ± 0.30 to 55.40 ± 0.14 Ma (Hirschmann et al. 1997). The U/Th ratios and rare earth element patterns in SH zircons are characteristic of magmatic partitioning, and, thus, we rule out the possibility that these are hydrothermal zircons. Additionally, the ferrodiorites in the vicinity of the SH all have magmatic and not hydrothermal textures, denying the possibility that zircons and sphenes crystallized from hydrothermal solutions. Temperature estimates of these rocks based on mineral equilibria are about 700°C (Xirouchakis et al. 2001), and Ti-in-zircon temperatures for sample 428-1 are $\sim 800^\circ\text{C}$ (Watson et al. 2006).

Late-Stage Gabbro Pegmatites and Sydtoppen Granophyre. Oxygen isotope analyses of fresh minerals in coarse-grained gabbroic pegmatites that occur locally throughout the intrusion also give information about other late-stage, hydrous differentiated melts. Analyses of zircon size fractions and other minerals in one sample of zircon-saturated pegmatite within lower zone b (SK-218) yielded $\delta^{18}\text{O}$ values of $4.2\text{‰} \pm 0.3\text{‰}$, in equilibrium with those of adjacent minerals but about $\sim 1\text{‰}$ lower than the estimated value for mantle zircon. It is noteworthy that the larger zircon size fraction in this sample is $\sim 0.5\text{‰}$ heavier than the smaller size fraction; this can be interpreted as reflecting progressive lowering of $\delta^{18}\text{O}$ melt during the interval of zircon crystallization. After adjusting for the melt-zircon fractionation at higher temperatures (e.g., fig. 3), this sample is only 0.8‰ – 0.5‰ depleted relative to the normal mantle. Another pegmatite from the MZ (sample SK-103; table 1) yielded $\delta^{18}\text{O}_{\text{Cpx}}$ values that are $\sim 0.6\text{‰}$ – 0.9‰ lower than those for the main volume Skaergaard $\delta^{18}\text{O}_{\text{Cpx}}$; this sample also yielded a relatively low $\delta^{18}\text{O}_{\text{Qtz}}$ value of 6.08‰ and a small $\Delta^{18}\text{O}[\text{qtz} - \text{amph}]$ value of 2.23‰ ; at equilibrium, the $\Delta^{18}\text{O}[\text{qtz} - \text{cpx}] = 1.72\text{‰}$ fractionation is consistent with a near-magmatic closure temperature. Two other likely examples of low- $\delta^{18}\text{O}$ gabbro pegmatite magmas with $\delta^{18}\text{O}_{\text{Cpx}}$ values of 3.5‰ and 4.1‰ are associated with fused xenoliths of gneiss in the MBS (Taylor and Forester 1979, their table 3, fig. 13);

these also would have been associated with late-stage low- $\delta^{18}\text{O}$ aqueous fluids. A very similar $\delta^{18}\text{O}$ zircon value is characteristic of the transitional granophyre of the Sydtoppen intrusion above the Basistoppen sill (table 1).

Discussion

Our new data show that the Skaergaard intrusion, during the later stages of its crystallization, evolved into a low- $\delta^{18}\text{O}$ melt. This reinterprets the intrusion's petrogenesis but requires an explanation for the origin of such a magma either as a product of magmatic fractionation or as the result of alteration by meteoric water that was somehow incorporated into these late-stage Fe-rich differentiates.

Radiogenic isotope studies of Skaergaard ferrodiorites and silicic rocks (Stewart and DePaolo 1990; McBirney and Creaser 2003) demonstrate that these differentiates are isotopically related to the underlying and overlying sequences and that assimilation of Archean gneisses could not have been an important factor in their petrogenesis. The main exception is the transgressive granophyres, which have a substantial component from the Archean basement (Hirschmann et al. 1997). Furthermore, the lack of any discontinuities in the regular progression of mineral compositions and trace-element concentrations in these highly evolved rocks indicates that this was not an intrusion of new magma; the low- $\delta^{18}\text{O}$ magmas must be the result of alteration of the existing, highly evolved ferrodiorites. Later intrusions, such as the Basistoppen sheet, which intrudes the UBS above the SH, were emplaced with normal $\delta^{18}\text{O}$ values (fig. 2). We discuss three hypotheses that might be capable of explaining the low- $\delta^{18}\text{O}$ oxygen in the late-stage Skaergaard ferrodiorite magmas, and we then consider their strengths and weaknesses.

Liquid Immiscibility as a Way to Generate Low- $\delta^{18}\text{O}$ Ferrodiorites: Extended differentiation of tholeiitic magmas normally leads to iron enrichment and silica depletion, followed by liquid immiscibility (e.g., McBirney and Nakamura 1973; Jakobsen et al. 2005; McBirney 2006; Veksler et al. 2007) that could possibly explain lower $\delta^{18}\text{O}$ values in Fe-rich ferrodiorites. The initiation of liquid immiscibility at UZc time or even earlier (Veksler et al. 2007) and the timing of ^{18}O depletion in the ferrodiorites seem more or less correct for this model. Our calculation, using CIPW norms and applying relevant fractionation factors for the most contrasting granophyre/melanogranophyre compositions published by Jakobsen et al. (2005), yields $\Delta^{18}\text{O}[\text{granophyre} - \text{melanogranophyre}] = 0.96\text{‰}$ at 1000°C (see fig. 3). This process can be thought

of as an isotopic difference between pyroxene + olivine-dominated (lower- $\delta^{18}\text{O}$) and feldspar \pm quartz-dominated (higher- $\delta^{18}\text{O}$) compounds or melts. The melanogranophyre melt needs to thoroughly exchange with and then be separated from a complementary more siliceous granophyre with a higher $\delta^{18}\text{O}$ value that reflects equilibrium mafic/silicic $^{18}\text{O}/^{16}\text{O}$ partitioning. In order to produce $>1\%$ lowering of $\delta^{18}\text{O}$ in melanogranophyre (a proxy for UZc ferrodiorites), the mass proportions of granophyre need to be significantly greater than those for melanogranophyre. In Skaergaard, the observed granophyres constitute at most $\sim 5\%$ of the UZ and UBS γ , and separation of even twice that amount would yield only $\sim 0.1\%$ depletion of ^{18}O in the residual ferrodiorite magma. However, if we postulate that these siliceous melts were actually much more abundant but were erupted (e.g., Hunter and Sparks 1987) after separation from the SH magma body, then this could, in theory, produce a significant ^{18}O depletion in the late-stage ferrodiorite magmas. Although a volcanic-plutonic connection may exist, by analogy with the low- $\delta^{18}\text{O}$ eruptive rocks of Iceland (e.g., Muehlenbachs et al. 1974; Gunnarsson et al. 1998; Bindeman et al. 2006), few, if any, silicic volcanic rocks are found near Skaergaard. Also, in Iceland, the rhyolites are commonly more depleted in ^{18}O than the coeval basalts, the reverse of what is required. In any case, even a relatively insignificant lowering of $\delta^{18}\text{O}$ by 0.5% requires eruption of several cubic kilometers of complementary rhyolite, for which there is simply no direct evidence.

Addition of Oxygen Derived from Meteoric Water to the Late-Stage Differentiates. The addition of some form of low- $\delta^{18}\text{O}$ oxygen derived from meteoric water is thus the most likely explanation of our results. We consider the following three plausible processes: (1) direct migration of meteoric water into Fe-rich residual melt (e.g., Friedman et al. 1974), (2) devolatilization of or exchange with fallen hydrated blocks (e.g., Taylor 1986), and (3) thermal metamorphism with remelting and recrystallization of subsolidus ferrodiorites after they were hydrothermally altered (this article).

1. Direct Migration of Water. The first explanation requires diffusion or advection of water into magma when the enclosing crystallized intrusion developed open cracks and significant fracture permeability. The latter seems certain to have occurred at Skaergaard, judging from the computer model of Norton and Taylor (1979), who showed that significant meteoric-hydrothermal flow was taking place both above and beneath the SH before final crystallization of the UZc-UBS γ magma lens.

While diffusion of water against an appreciable temperature gradient is problematic, the residual $\sim 750\text{--}800\text{C}$ melt lens may have been virtually isothermal with neighboring hot, solid, water-saturated gabbros above and below. However, another problem is that the fracture-dominated meteoric-hydrothermal system is under hydrostatic pressure, whereas the magma body is presumably subjected to a significantly higher lithostatic pressure. Thus, an isothermal chemical gradient around the evolved, water-undersaturated melt would have to drive the water from the meteoric water-saturated, earlier-crystallized Skaergaard rocks up a pressure gradient and into the residual magma. This requires diffusion of large amounts of water from the external fracture system into the magma body, through a ductile boundary layer of unknown thickness. In order to achieve lowering of the bulk $\delta^{18}\text{O}$ magma values by 1% – 2% , it would take 4–8 wt% water with unshifted low- $\delta^{18}\text{O}$ values of -12% . At least two to 10 times more water is required if we substitute a more plausible, strongly ^{18}O -shifted aqueous fluid with $\delta^{18}\text{O} = -5\%$ to $+4\%$ (see figs. 31, 33 in Norton and Taylor 1979). These required water concentrations far exceed limits for water solubility in such melts at the relatively low $\sim 0.5\text{--}1.0\text{--}3.3 \pm 1.3\text{-kb}$ Skaergaard crystallization pressures (McBirney 1996; Larsen and Tegner 2006). This may be a possibility for the deeper, late-stage, amphibole-bearing pegmatites SK-218 and SK-103, which exhibit only a subtle $\sim 0.5\%$ ^{18}O depletion. While accessory ferroamphibole is present in the SH, its amount is small, and the estimated amount of water in the SH and surrounding rocks is $<1\text{--}2\text{ wt}\%$. We conclude that direct addition of external low- $\delta^{18}\text{O}$ water is an inefficient and problematic process not supported by the characteristically anhydrous Skaergaard mineral assemblages and not sufficient to produce the required depletion in ^{18}O .

2. "Self-Fertilization" Model for the UZc-UBS γ Magmas. The low- $\delta^{18}\text{O}$ magmas at Skaergaard can, in principle, be formed by a process that we term "self-fertilization" (Bindeman et al. 2008b). This would occur either by exchange with fallen hydrothermally altered rocks from the overlying, earlier-crystallized middlemost upper border series (UBS β) and UBS γ (fig. 5A) or by disaggregation of blocks into smaller pieces and constituent minerals when these water-saturated rocks sank through magma (fig. 5B). This could introduce low- $\delta^{18}\text{O}$ meteoric water and crystals into the Skaergaard differentiated magma. If sufficient water is added to saturate the melt, then some water might escape back into the surrounding hydrothermal system,

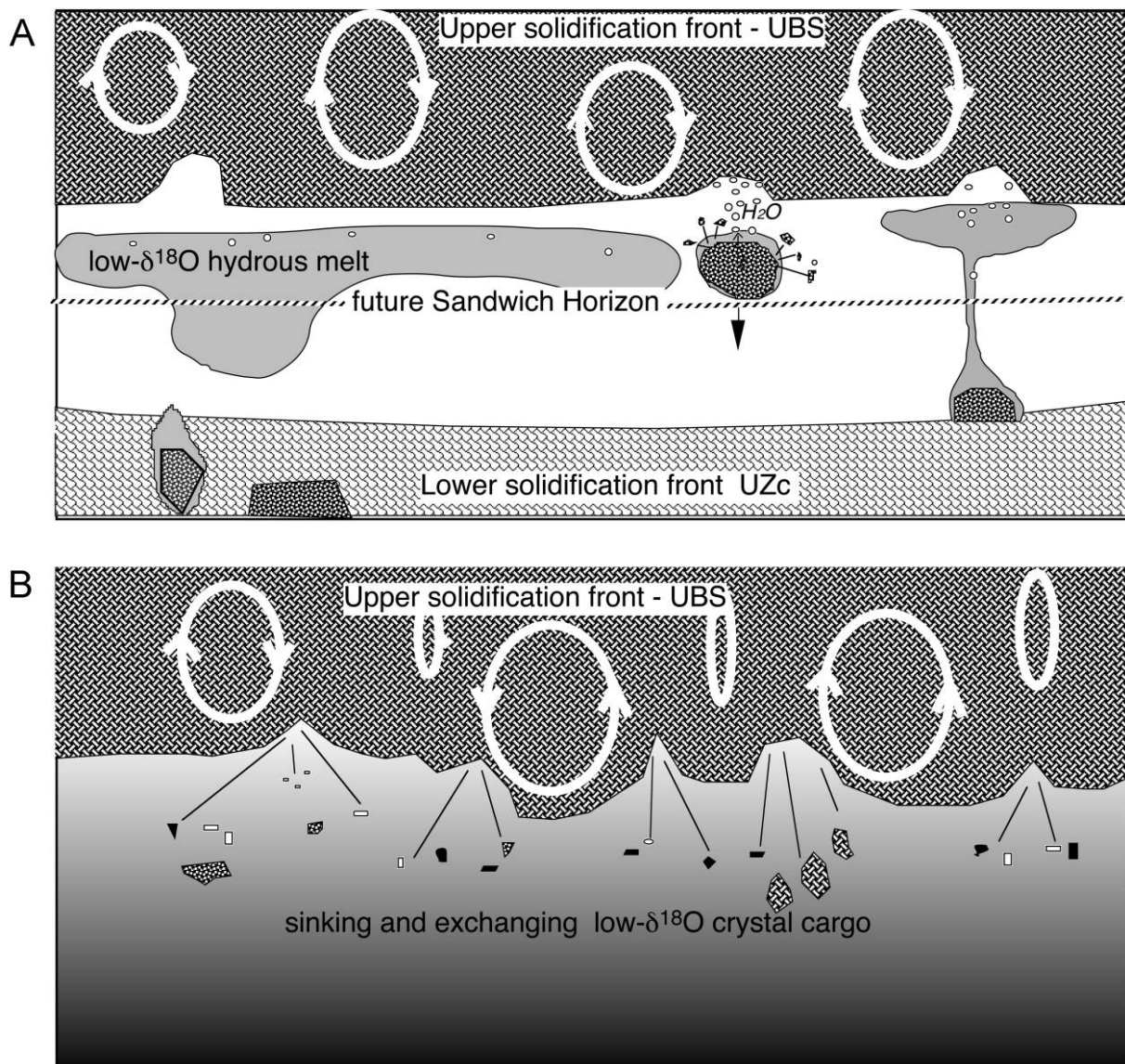


Figure 5. Hypothetical mechanisms for production of low- $\delta^{18}\text{O}$ magmas during final stages of crystallization of the Skaergaard intrusion. *A*, Sequestration of low- $\delta^{18}\text{O}$ fluid/hydrous melt derived from fallen hydrothermally altered upper border series blocks; the low- $\delta^{18}\text{O}$ melts coalesce and pond just beneath the upper crystallization boundary because of density stratification, possibly leading to water bubble escape into the upper hydrothermal system. *B*, Cartoon depicting interactions between the lens of late-stage ferrodiorite magma and low- $\delta^{18}\text{O}$ melts and crystals derived from the overlying upper border series rocks. Disruption and fragmentation of hydrothermally altered roof rocks causes rapid dispersion of low- $\delta^{18}\text{O}$ melt blebs and crystals within the magma lens; the fine-grained nature of the shattered materials facilitates oxygen isotope exchange with the ferrodiorite magma. We suggest that such processes may characterize shallow intrusions such as Skaergaard, in which meteoric pore fluid expansion can occur catastrophically, based on the *T-V* properties of water at low pressure and irregularities in the stress patterns and temperature distributions

but it would nevertheless have left its low- $\delta^{18}\text{O}$ imprint on the magma.

Dehydration and exchange with hydrothermally altered blocks from the UBS and roof rocks (figs. 1, 5A) is the only process that we are certain added meteoric water oxygen and caused local ^{18}O depletion of the Skaergaard magma. This is best

documented by a 6-m-wide basaltic xenolith in MZ that was studied by Taylor and Forester (1979, their figs. 16, 17). The center of this block has $\delta^{18}\text{O} = -4.0\text{‰}$, and the enclosing gabbro >2 m away crystallized from MZ magma that had $\delta^{18}\text{O}$ very close to the primary mantle value of $+5.5\text{‰}$. However, outer parts of the xenolith have

$\delta^{18}\text{O} = -1.5\text{‰}$ to $+2.3\text{‰}$, and the immediately adjacent MZ gabbro crystallized from a low- $\delta^{18}\text{O}$ melt that was at least 2.5‰ depleted in ^{18}O compared with the surrounding MZ magma reservoir. In other words, there was an exchange of oxygen between this block and the surrounding melt, with the block becoming higher in $\delta^{18}\text{O}$ and the rind of melt undergoing depletion in ^{18}O . A similar 2-m-wide basaltic xenolith from the MBS has $\delta^{18}\text{O} = 1.2\text{‰}$. Sonnenenthal and McBirney (1998) have described the reaction-transport mechanisms that could have been responsible for this exchange.

Basaltic xenoliths of this kind are quite rare and thus by themselves cannot be responsible for any major $\delta^{18}\text{O}$ changes in the Skaergaard magmas. None has been found in the vicinity of the SH. However, they nicely illustrate the mechanism of $\delta^{18}\text{O}$ exchange that accompanied their thermal metamorphism (e.g., pyroxene replacing amphibole and micas, feldspar crystals becoming less cloudy, and formation of more iron-rich rims around the fallen blocks, indicative of water migrating outward). Note that the exchange mechanism is not simply removal of water from the xenolith—there also must be two-way diffusive exchange of $^{18}\text{O}/^{16}\text{O}$ between the minerals in the xenolith and the surrounding melt, presumably enhanced by diffusion through the interconnected aqueous fluid film that would permeate grain boundaries and fractures.

In striking contrast to the rarity of basalt xenoliths, fallen blocks (autoliths) from the earlier-crystallized UBS roof sequence are abundant throughout the central parts of the layered series, making up perhaps as much as 2% of the intrusion (Irvine et al. 1998). Given the rather large size of the UBS blocks, some of which are more than 100 m in diameter, their fall through the magma chamber is expected to have been rather rapid relative to their heating, so most of their water was released after they reached the solidification zone on the floor (e.g., Sonnenenthal and McBirney 1998). Owing to the high ($>600^\circ\text{C}$) temperatures, the rock-water oxygen isotope fractionations would be very small ($\sim 0\text{‰} \pm 1\text{‰}$), and the released water would approximate either the bulk $\delta^{18}\text{O}$ values of the hydrothermally altered rocks themselves or the even lower $\delta^{18}\text{O}$ values of any water that may have been present in their pores and fractures. Many of these autoliths were analyzed by Taylor and Forester (1979), and they were invariably found to be lower in ^{18}O than the layered gabbros a few meters away but commonly by less than 0.5‰ – 1.0‰ . Thus, as in the case of the basaltic xenoliths, there is no doubt that there was also $^{18}\text{O}/^{16}\text{O}$ exchange between the

autoliths and the contemporaneous Skaergaard magma. However, the problem now becomes one of material balance, namely, (a) What are the respective volumes of magma and stoped blocks, and what kinds of $^{18}\text{O}/^{16}\text{O}$ changes might occur in the magma reservoir? and (b) Why are there no measurable depletions in ^{18}O observed in the bulk Skaergaard magma until UZc-UBS γ time?

The second question is actually very easy to answer, given the huge volume of the Skaergaard magma chamber and the known facts that the autoliths (i) are typically only 0.5‰ – 1.0‰ lower in $\delta^{18}\text{O}$ than the surrounding gabbro and (ii) make up no more than 1%–2% of the intrusion by volume (i.e., $3\text{--}6\text{ km}^3$). Let us suppose that all of these autoliths started out with absurdly low $\delta^{18}\text{O}$ values of -1.5‰ to -2.0‰ (i.e., equal to the lowest values of any UBS samples analyzed by Taylor and Forester [1979]) and that they were then all enriched in ^{18}O by 6‰ – 8‰ after falling to the floor of the chamber. In this scenario, at MZ time, after 50% crystallization had reduced the magma volume to $\sim 150\text{ km}^3$, the maximum change in the remaining magma reservoir would be $<0.3\text{‰}$. If more plausible starting values and more reasonable $\delta^{18}\text{O}$ shifts in the autoliths are used, this putative change in the bulk magma is reduced to an essentially unmeasurable 0.01‰ – 0.1‰ .

With continued crystallization, as the magma volume becomes progressively smaller, the material balance problem becomes less serious. Obviously, it is far easier to produce a 1.5‰ $\delta^{18}\text{O}$ depletion in a 30-m-thick magma sheet than in a magma body 150 km^3 in size. Fewer fallen blocks would be required because by UZc time, the external hydrothermal system had been operating for more than 100,000 yr (Norton and Taylor 1979) and the UBS roof rocks were now thoroughly altered, with much lower $\delta^{18}\text{O}$ values (26 UBS samples have a mean $\delta^{18}\text{O}_{\text{plag}} = 1.9\text{‰}$, compared with a mean value of 4.5‰ for the seven MZ autoliths; Taylor and Forester 1979). This possibility seems unlikely, however, because virtually no blocks of any kind have been recognized in the uppermost parts of the layered series.

Clearly, self-fertilization at Skaergaard can locally produce small packets of low- $\delta^{18}\text{O}$ magma. However, our problem is how we might produce at least a 30-m-thick sheet of such a magma in the vicinity of the SH. Is there some way to concentrate these low- $\delta^{18}\text{O}$ melts together at the top of the magma chamber? Essentially every autolith or xenolith that was earlier incorporated into the HZ, LZ, MZ, UZa, and UZb would have been surrounded by a carapace of low- $\delta^{18}\text{O}$ interstitial

melt. If these hydrous melts were more buoyant than the adjacent bulk magma reservoir and if they could be concentrated into a coherent package, then each of these individual packets conceivably might rise as plumes without losing their integrity until they reached the magma roof. Here they could pond and coalesce, confined by density stratification (fig. 5A). A simple material-balance calculation indicates that the known quantities of blocks could thereby produce a sufficient amount of low- $\delta^{18}\text{O}$ magma. A small degree of partial melting of the blocks could add low-density silicates to the hydrous magma packets, adding to their buoyancy. However, as Sonnenthal and McBirney (1998) have shown, the adjacent gabbros were strongly enriched in iron and titanium from the blocks, which argues against the idea that such magma packets would have been buoyant. They concluded that the felsic interstitial liquid adjacent to the blocks diffused inward to replace the lost mafic components, transforming the blocks into anorthosite by volume-for-volume metasomatic replacement.

A possible variation on this same theme may be $^{18}\text{O}/^{16}\text{O}$ exchange and release of water from the blocks very near the roof of the intrusion immediately after they became detached (fig. 5B). Although much of this probably occurs during metamorphism of hydrous minerals on the floor of the intrusion (e.g., Sonnenthal and McBirney 1998; McBirney and Creaser 2003), the low- $\delta^{18}\text{O}$ aqueous fluid in fractures and pores in the blocks conceivably could be released much earlier, perhaps explosively. Again, any low- $\delta^{18}\text{O}$ melt formed in this way would have to accumulate in a density-stratified layer just under the roof and not undergo back-mixing into the bulk magma reservoir.

In either of these hypothetical scenarios, sequestration of low-density, low- $\delta^{18}\text{O}$ material near the roof would be happening throughout UZ time while the UZa and UZb ferrogabbros were crystallizing on the floor and roof of the intrusion, with normal MORB $\delta^{18}\text{O}$ values. However, what is happening to the rocks that are chemically and mineralogically equivalent to UZa and UZb and are simultaneously crystallizing as UBS γ along the roof of the magma chamber? Logically, one would expect that these UBS γ rocks would have crystallized from the hypothetical low- $\delta^{18}\text{O}$ magma that is accumulating just beneath the roof. This should lead to a geometrical asymmetry in the distribution of low- $\delta^{18}\text{O}$ rocks, with all of UBS γ having formed from such a melt, whereas this would be delayed in the layered series until earliest UZc time or even later. In fact, our new data indicate that the lower part of UBS γ is depleted even more than the SH, as is shown by

zircons with $\delta^{18}\text{O} = 2\%$ in sample KG-423. Unfortunately, only two samples from the upper part of UBS γ are available to test this idea (KG-253, which is the most ^{18}O -depleted sample lying within the anomalous UZc-UBS γ array in fig. 13 of Taylor and Forester 1979, and newly analyzed low- $\delta^{18}\text{O}$ sample SK-336, which contains noninverted clinopyroxene). Depending on how one interprets this anomalous $\delta^{18}\text{O}$ plagioclase- $\delta^{18}\text{O}$ clinopyroxene array, it is possible to conclude that KG-253 crystallized from a ferrodiorite melt with an extremely low $\delta^{18}\text{O}$ value of $2.2\% \pm 0.7\%$ and SK-336 from a melt with $\delta^{18}\text{O} \sim 3.5\%$, implying that just underneath the roof of the magma chamber, significant quantities of low- $\delta^{18}\text{O}$ melt may have been forming as early as uppermost UZa time. Although the available data are therefore compatible with the proposed model of $^{18}\text{O}/^{16}\text{O}$ asymmetry, this obviously needs confirmation by further sampling of UBS γ and UBS β . Note that it was during UBS β time that by far the largest accumulation of blocks occurred in the Skaergaard layered series, so a more detailed search for low- $\delta^{18}\text{O}$ magmas in UBS β is particularly important.

Alternatively, the self-fertilization activity at Skaergaard may have been dominated by a process that included aqueous fluid expansion (fig. 5B), leading to dispersal of low- $\delta^{18}\text{O}$ crystals and melt blebs into the lens of ferrodiorite magma. This view is supported by the fact that the hydrothermal system was operating vigorously only a couple of meters away from (i.e., above and below) the UZc-UBS γ magma body ($>650^\circ\text{C}$; Norton and Taylor 1979). The UZc-UBS γ lens of magma thus may have contained dispersed low- $\delta^{18}\text{O}$ fragments and autocrysts whose finer grain size would have facilitated $^{18}\text{O}/^{16}\text{O}$ exchange with the melt. Incorporation of such materials would have accelerated crystallization of similar minerals, and the autolith crystals would have blended with newly crystallized minerals, all contributing to the perhaps heterogeneous low- $\delta^{18}\text{O}$ crystalline cargo. Finally, late crystallization of low- $\delta^{18}\text{O}$ accessory sphene and zircon could have proceeded from a true, interstitial low- $\delta^{18}\text{O}$ melt. This process seems unlikely, however, because we find no petrographic evidence for these autolith crystals, and the fallen blocks are solid and coherent, with no signs of disaggregation.

3. Thermal Metamorphism and Remelting by Subsequent Intrusions. The majority of low- $\delta^{18}\text{O}$ igneous rocks around the world appear to have been produced by remelting of hydrothermally altered rocks that have undergone lowering of their $^{18}\text{O}/^{16}\text{O}$ ratio by subsolidus exchange with meteoric waters (e.g., Taylor 1986; Gunnarsson et al. 1998;

Bindeman et al. 2006, 2008a). Can such a process also characterize Skaergaard, and, in particular, is it possible that the late-stage, lowest-temperature ferrodiorites around the SH crystallized, then became hydrothermally altered by meteoric waters, and finally were reheated, recrystallized, and partially remelted by a new intrusion of hot basaltic magma (fig. 6)? The only known large basaltic intrusion that is close in time and space to the crystallization of the SH is the 660-m-thick Basistoppen sill, emplaced 150–200 m above the SH. It was intruded at 1150°–1200°C, supposedly while the UBS was still quite hot, and there is evidence of local remelting, back-veining, and hybridization, particularly at its lower contact with UBS γ (Naslund 1986). Skaergaard igneous layering and Basistoppen contacts are sub-parallel and were later tilted together, also suggesting nearly concurrent emplacement.

The Basistoppen magma sheet would have formed an impermeable barrier to the hydrothermal flow system. This barrier would have stretched across the upper part of the intrusion (figs. 1, 6) and would have suddenly interrupted any upwardly buoyant hydrothermal plume that might have been operating in the UBS after final SH crystallization. The hydrothermal system in the UBS γ rocks underneath this magma sheet conceivably could break up into numerous convection cells that could transfer heat much more efficiently than simple thermal conduction. The whole zone might remain at quite a high temperature until the Basistoppen sheet finally crystallized and then fractured, after which the flow system could revert to its pre-Basistoppen form (Norton and Taylor 1979). At a plausible crystallization rate of 3 cm/yr, this could take as long as 20,000 yr.

It is interesting to speculate that because of the intimate contact of the SH with this vigorous hydrothermal system, remelting of the SH could have occurred under higher H₂O fugacities and hence lower temperatures (~940°C) than its initial crystallization (Lindsley et al. 1969). As shown by the graphs of depth versus temperature, solidus temperature, and MgO content (fig. 6), it is plausible that remelting processes of varying intensity (i.e., crystal/melt ratio) could have affected the entire section of UBS γ between the SH and the Basistoppen intrusion, perhaps even being concentrated in the vicinity of the SH. Well-defined remelting zones up to 5 m thick are observed in outcrops of UBS γ at the lower contact of the Basistoppen sill (Naslund 1986). Among the complexities that need to be explained in these ferrodiorites, however, are the preservation of very fine-grained inversion-exsolution textures in many of the pyrox-

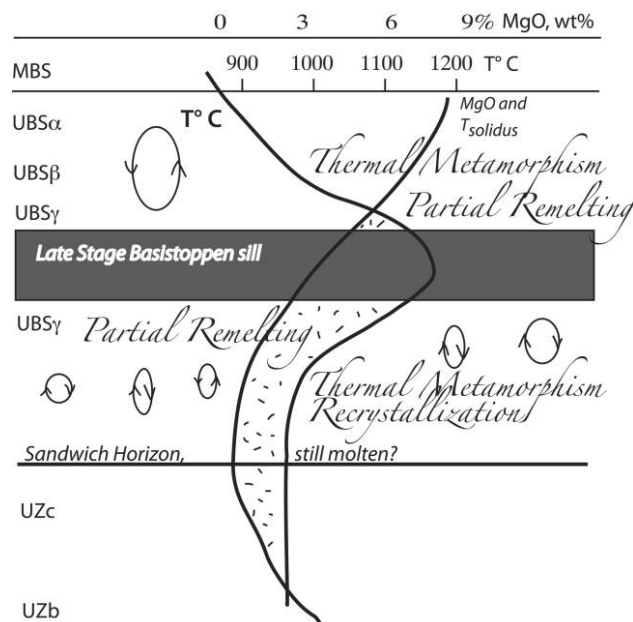


Figure 6. Schematic representation of possible thermal effects of Basistoppen sill intrusion on metamorphism, recrystallization, and remelting of already crystallized and hydrothermally altered portions of the lowermost part of the upper border series (UBS γ), the Sandwich Horizon, and the uppermost part of the layered series (UZc) as a mechanism to generate low- $\delta^{18}\text{O}$ melts. Drawing is not to scale; it depicts disruption of the pre-Basistoppen meteoric-hydrothermal system into multiple cells, as well as a greater remelting potential for the most differentiated, Mg-poor ferrodiorites near the Sandwich Horizon. The stippled pattern between the two curves denotes parts of the intrusion in which the temperature increase due to Basistoppen intrusion will exceed the temperature of the local solidus; this is characteristic of most-differentiated, Fe-rich portions of the intrusion in which groundmass would remelt first during heating. Inverted mosaic pyroxenes would recrystallize (see appendix in the online edition or from the *Journal of Geology* office).

enes (ferrobustamite-hedenbergite) and the occurrence of samples with and without inverted clinopyroxenes, often in close proximity (table 1).

One might infer that these textural features actually support the reheating and remelting process: a significant proportion of the UZc-UBS γ rocks (exemplified by samples SK-15, SK-333, and SK-336 in this study) contain uninverted crystals of hedenbergite, and some contain both inverted and uninverted clinopyroxenes (e.g., SK-332). What kind of process could have led to such a variety of end products? Consider what happens when a typical UZc-UBS γ liquid crystallizes its characteristic assemblage of fayalitic olivine + quartz + plagioclase together

with ferrobustamite. On cooling, the latter inverts, producing a very fine-grained mosaic of hedenbergite grains that become even more Ca-rich with decreasing temperature (McBirney 2006, fig. 4-11e, p. 133). These Ca-rich compositions would be stable at higher temperatures in any reheating process during which hedenbergite is unlikely to reinvert to the high-temperature form (see phase diagram in the appendix in the online edition or from the *Journal of Geology* office). In the presence of minor amounts of melt, the larger grains would grow at the expense of smaller ones, and in this way, the mosaic texture would be replaced by one with larger crystals of hedenbergite. One could even argue that any UZc-UBS γ rock without inverted pyroxene must have been reheated, recrystallized, and perhaps partly remelted.

One might speculate that UZc-UBS γ rocks containing just large individual grains of hedenbergite and without any inverted pyroxene mosaics may have been recrystallized or only partly melted, whereas those that were more completely melted would have gone through the crystallization cycle a second time (see appendix), leading to the characteristic inversion textures seen in such ferrodiorites. If valid, this would suggest that, relative to the Basistoppen sill, the more distal samples would tend to be the partial melts (such as SK-15), whereas many of the proximal samples would have greater melt/solid ratios. Samples with both kinds of pyroxenes would be intermediate between these two end members. We visualize that the zones with varying degrees of melting might be very heterogeneously distributed beneath the Basistoppen sill because of vagaries in composition, particularly water content. The distribution and proportions of OH-bearing minerals in these rocks just before their remelting would depend to a large degree on the fractures that existed in these rocks because these were the main conduits for the hydrothermal fluids. The intensity of fracturing need not bear any obvious geometrical relationship to the Basistoppen sill, but it surely would help determine the zones where melting would be initiated.

Regardless of what explanation is finally accepted to explain the development of the late-stage low- $\delta^{18}\text{O}$ magmas, we feel certain that it will involve remelting by the Basistoppen sill, devolatilization and exchange between the magma and the disaggregated fragments of the UBS, or both. We term the latter process "self-fertilization" because it all happened inside the intrusion and involved oxygen from the meteoric-hydrothermal system that was being driven by the intrusion itself. These interactions with the fallen UBS fragments added

H_2O to the magma, changed isotopic and trace-element distributions, and fertilized the residual, unsolidified, more differentiated portions of the intrusion. Self-fertilization by exchange with hydrated fallen blocks or with dispersed hydrothermally altered crystalline cargo may have contributed to the rapid increase in the F/Cl ratio above MZ. The F/Cl ratio of apatite remains constant throughout LZ and most of the MZ but then increases dramatically from there up to the SH (Sonnenthal 1990). This is attributed to exsolution of a hydrous vapor phase that would remove chlorine while leaving fluorine in the silicate melt.

The oxygen isotopic anomalies observed during this study indicate that the horizon with the greatest concentrations of incompatible trace elements yet found in the entire intrusion (termed the Brooks Horizon) also has the lowest observed magmatic $\delta^{18}\text{O}$ values. The asymmetric distribution of trace elements may need to be interpreted in view of the possible asymmetry that seems to exist in the distribution of low- $\delta^{18}\text{O}$ magmas above and below the SH.

Where Do We Go from Here? It is critical to find out whether the zone of low- $\delta^{18}\text{O}$ melts surrounding the SH was only ~30 m thick or whether it included all of UZc and perhaps all of UBS γ . In other words, was there an $^{18}\text{O}/^{16}\text{O}$ asymmetry between the UZa and UZb liquids and the time-equivalent liquids in the upper part of UBS? Could this asymmetry be attributed to the metamorphic effects of the Basistoppen sill, which was emplaced into the upper part of UBS γ and may have partially remelted the most water-rich, lowest-solidus zones in this section of UBS? These questions can be answered only by more field studies and by gathering (a) large zircon-bearing samples suitable for accessory mineral extraction and (b) a suite of samples with a variety of textural relationships involving both inverted and uninverted clinopyroxenes. At the same time, there should be further studies of the physics of whether a water-rich, density-stratified, low- $\delta^{18}\text{O}$ magma layer could continuously accumulate underneath the roof of Skaergaard and similar intrusions. Then, one would have to show that this layer could be preserved and not be dispersed back into the bulk magma reservoir until the time of final crystallization of UZc-UBS γ and SH ferrodiorites.

It should be pointed out that even if the entire UZc-UBS γ sequence can be proved to have formed from a low- $\delta^{18}\text{O}$ magma, the volume of such a magma is minuscule compared with the gigantic volumes of low- $\delta^{18}\text{O}$ magmas (both rhyolite and basalt) that have been erupted in other areas on Earth, notably in Iceland and Yellowstone National

Park (e.g., Muehlenbachs et al. 1974; Hildreth et al. 1984; Taylor 1986; Gunnarsson et al. 1998; Bindeman et al. 2006, 2008a). Although interaction with and/or partial melting of hydrothermally altered roof rocks is the favored explanation in all of these other occurrences, Skaergaard may be one of our best places to test this model because nowhere else are the geology, geochemistry, and petrology so well documented and so tightly constrained. Note, however, that these types of self-fertilization processes probably cannot generate large volumes of low- $\delta^{18}\text{O}$ magma. Furthermore, we certainly need to revisit the idea that the Basistoppen sill might be responsible for partial remelting of UZc and much of UBS γ (e.g., fig. 6).

ACKNOWLEDGMENTS

We thank R. Larsen (Technical University, Trondheim, Norway) for the sample of pegmatite from the lower zone and T. Nielsen (Geological Survey of Denmark and Greenland) for help in extracting the picrite from the Danish Lithosphere Center collections in Copenhagen. M. Hamilton (University of Toronto) is thanked for supplying mineral separate from the Sandwich Horizon. D. Naslund is thanked for fruitful discussions on Skaergaard geology and sample donation. I. Veksler and an anonymous reviewer are thanked for their fruitful reviews. Analyses were supported by National Science Foundation grant EAR-0537872 to I. N. Bindeman.

REFERENCES CITED

- Anderson, A. T., Jr.; Clayton, R. N.; and Mayeda, T. K. 1971. Oxygen isotope geothermometry of mafic igneous rocks. *J. Geol.* 79:715–729.
- Bindeman, I. N.; Fu, B.; Kita, N.; and Valley, J. W. 2008a. Origin and evolution of Yellowstone silicic magmatism based on ion microprobe analysis of isotopically zoned zircons. *J. Petrol.* 49:163–193.
- Bindeman, I. N.; Gurenko, A. A.; Sigmarsson, O.; and Chaussidon, M. 2008b. Oxygen isotope heterogeneity and disequilibria of olivine crystals in large volume Holocene basalts from Iceland: evidence for magmatic digestion and erosion of Pleistocene hyaloclastites. *Geochim. Cosmochim. Acta* 72:4397–4420.
- Bindeman, I. N.; Ponomareva, V. V.; Bailey, J. C.; and Valley, J. W. 2004. Kamchatka Peninsula: a province with high- $\delta^{18}\text{O}$ magma sources and large-scale $^{18}\text{O}/^{16}\text{O}$ depletion of the upper crust. *Geochim. Cosmochim. Acta* 68:841–865.
- Bindeman, I. N.; Sigmarsson, O.; and Eiler, J. M. 2006. Time constraints on the origin of large volume low- $\delta^{18}\text{O}$ basalts derived from O-isotope and trace element mineral zoning and U-series disequilibria in the Laki and Grimsvotn volcanic system, Iceland. *Earth Planet. Sci. Lett.* 245:245–259.
- Blank, H. R., and Gettings, M. E. 1973. Subsurface form and extent of the Skaergaard intrusion, East Greenland. *EOS: Trans. Am. Geophys. Union* 54:507.
- Brooks, C. K. 1969. On the distribution of zirconium and hafnium in the Skaergaard intrusion, East Greenland. *Geochim. Cosmochim. Acta* 33:357–374.
- Brooks, C. K.; Keays, R. R.; Lambert, D. D.; Frick, L. R.; and Nielsen, T. F. D. 1999. Re-Os isotope geochemistry of Tertiary picritic and basaltic magmatism of East Greenland: constraints on plume-lithosphere interactions and the genesis of the Platinova reef, Skaergaard intrusion. *Lithos* 47:107–126.
- Brooks, C. K.; Larsen, L. M.; and Nielsen, T. F. D. 1991. Importance of iron-rich tholeiitic magmas at divergent plate margins: a reappraisal. *Geology* 19:269–272.
- Brooks, C. K., and Nielsen, T. F. D. 1990. The differentiation of the Skaergaard intrusion: a discussion of Hunter and Sparks (Contrib. Mineral. Petrol. 95:451–461). *Contrib. Mineral. Petrol.* 104:244–247.
- Chiba, H.; Chacko, T.; Clayton, R. N.; and Goldsmith, J. R. 1989. Oxygen isotope fractionations involving diopside, forsterite, magnetite, and calcite: application to geothermometry. *Geochim. Cosmochim. Acta* 53:2985–2995.
- Eiler, J. M. 2001. Oxygen isotope variations in basaltic lavas and upper mantle rocks. *Rev. Mineral. Geochem.* 43:319–364.
- Friedman, I.; Lipman, P. W.; Obradovich, J. D.; Gleason, J. D.; and Christiansen, R. L. 1974. Meteoric water in magmas. *Science* 184:1069–1072.
- Gunnarsson, B.; Marsh, B. D.; and Taylor, H. P., Jr. 1998. Generation of Icelandic rhyolites: silicic lavas from the Torfajökull central volcano. *J. Volcanol. Geotherm. Res.* 83:1–45.
- Hamilton, M. A., and Brooks, C. K. 2004. A precise U-Pb zircon age for the Skaergaard intrusion. *Geochim. Cosmochim. Acta* 68:A587–A587.
- Hildreth, W.; Christiansen, R. L.; and O'Neil, J. R. 1984. Catastrophic isotopic modification of rhyolitic magma at times of caldera subsidence, Yellowstone Plateau volcanic field. *J. Geophys. Res.* 89:8339–8369.
- Hirschmann, M. M.; Renne, P. R.; and McBirney, A. R. 1997. $^{40}\text{Ar}/^{39}\text{Ar}$ dating of the Skaergaard intrusion. *Earth Planet. Sci. Lett.* 146:645–658.
- Hunter, R. H., and Sparks, R. S. J. 1987. The differentiation of the Skaergaard intrusion. *Contrib. Mineral. Petrol.* 95:451–461.
- Irvine, T. N.; Andersen, J. C. O.; and Brooks, C. K. 1998. Included blocks (and blocks within blocks) in the Skaergaard intrusion: geologic relations and the origins of rhythmic modally graded layers. *Geol. Soc. Am. Bull.* 110:1398–1447.
- Jakobsen, J. K.; Veksler, I. V.; Tegner, C.; and Brooks, C. K. 2005. Immiscible iron- and silica-rich melts in basalt

- petrogenesis documented in the Skaergaard intrusion. *Geology* 33:885–888.
- Larsen, L. M.; Watt, W. S.; and Watt, M. 1989. Geology and petrology of the Lower Tertiary plateau basalts of the Scoresby Sund region, East Greenland. *Bull. Grøn. Geol. Unders.* 157:1–164.
- Larsen, R. B., and Brooks, C. K. 1994. Origin and evolution of gabbroic pegmatites in the Skaergaard intrusion, East Greenland. *J. Petrol.* 35:1651–1679.
- Larsen, R. B., and Tegner, C. 2006. Pressure conditions for the solidification of the Skaergaard intrusion: eruption of East Greenland flood basalts in less than 300,000 years. *Lithos* 92:181–197.
- Lindsley, D. H.; Brown, G. M.; and Muir, I. D. 1969. Conditions of the ferrowollastonite-ferrohedenbergite inversion in the Skaergaard intrusion, East Greenland. *Mineral. Soc. Am. Spec. Publ.* 2:193–201.
- McBirney, A. R. 1995. Mechanisms of differentiation in the Skaergaard intrusion. *J. Geol. Soc. Lond.* 152:421–435.
- . 1996. The Skaergaard intrusion. *In* Cawthorn, R. G., ed. *Layered intrusions*. Amsterdam, Elsevier Science, p. 147–180.
- . 2002. Skaergaard layered series. VI. Excluded trace elements. *J. Petrol.* 43:535–556.
- . 2006. *Igneous petrology* (3rd ed.). Sudbury, MA, Jones & Bartlett, 550 p.
- McBirney, A. R., and Creaser, R. A. 2003. The Skaergaard layered series. VII. Sr and Nd isotopes. *J. Petrol.* 44:757–771.
- McBirney, A. R., and Nakamura, Y. 1973. Immiscibility in late-stage magmas of the Skaergaard intrusion. *Carnegie Inst. Wash. Year Book* 72:348–352.
- McBirney, A. R., and Naslund, H. R. 1990. The differentiation of the Skaergaard intrusion: a discussion of Hunter and Sparks (*Contrib. Miner. Petrol.* 95: 451–461). *Contrib. Mineral. Petrol.* 104:235–240.
- McBirney, A. R., and Noyes, R. M. 1979. Crystallization and layering of the Skaergaard intrusion. *J. Petrol.* 20:487–554.
- Morse, S. A. 1990. The differentiation of the Skaergaard Intrusion: a discussion of Hunter and Sparks (*Contrib. Mineral. Petrol.* 95: 451–461). *Contrib. Mineral. Petrol.* 104:240–244.
- Muehlenbachs, K.; Anderson, A. T.; and Sigvaldason, G. E. 1974. Low-¹⁸O basalts from Iceland. *Geochim. Cosmochim. Acta* 38:587–588.
- Naslund, H. R. 1986. Disequilibrium partial melting and rheomorphic layer formation in the contact aureole of the Basistoppen sill. *Contrib. Mineral. Petrol.* 93:359–367.
- Nielsen, T. F. D. 2004. The shape and volume of the Skaergaard intrusion, Greenland: implications for mass balance and bulk composition. *J. Petrol.* 45:507–530.
- Nielsen, T. F. D.; Andersen, J. C. Ø.; and Brooks, C. K. 2005. The Platinova reef of the Skaergaard intrusion. *In* Mungall, J. E., ed. *Exploration for platinum group element deposits*. Mineral. Assoc. Can. Short Course Notes 35:431–455.
- Norton, D., and Taylor, H. P., Jr. 1979. Quantitative simulation of the hydrothermal systems of crystallizing magmas on the basis of transport theory and oxygen isotope data: an analysis of the Skaergaard intrusion. *J. Petrol.* 20:421–486.
- O'Neil, J. R., and Taylor, H. P., Jr. 1967. The oxygen isotope and cation exchange chemistry of feldspars. *Am. Mineral.* 52:1414–1437.
- Sonnenthal, E. L. 1990. Metasomatic replacement and the behavior of fluorine and chlorine during differentiation of the Skaergaard intrusion, East Greenland. PhD dissertation, University of Oregon, Eugene.
- Sonnenthal, E. L., and McBirney, A. R. 1998. The Skaergaard layered series. IV. Reaction-transport simulations of foundered blocks. *J. Petrol.* 39:633–661.
- Stewart, B. W., and DePaolo, D. J. 1990. Isotopic studies of processes in mafic magma chambers. II. The Skaergaard intrusion, East Greenland. *Contrib. Mineral. Petrol.* 104:125–141.
- Taylor, H. P., Jr. 1968. The oxygen isotope geochemistry of igneous rocks. *Contrib. Mineral. Petrol.* 19:1–71.
- . 1986. Igneous rocks. II. Isotopic case studies of circum-Pacific magmatism. *In* Valley, J. W.; Taylor, H. P., Jr.; and O'Neil, J. R., eds. *Stable isotopes in high-temperature geological processes*. *Rev. Mineral.* 16: 217–317.
- Taylor, H. P., Jr., and Epstein, S. 1963. O¹⁸/O¹⁶ ratios in rocks and coexisting minerals of the Skaergaard intrusion. *J. Petrol.* 4:51–74.
- Taylor, H. P., Jr., and Forester, R. W. 1979. An oxygen and hydrogen isotopic study of the Skaergaard intrusion and its country rocks: a description of a 55-Ma fossil hydrothermal system. *J. Petrol.* 20:355–419.
- Valley, J. W. 2003. Oxygen isotopes in zircon. *Rev. Mineral. Geochem.* 53:343–385.
- Valley, J. W.; Bindeman, I. N.; and Peck, W. H. 2003. Calibration of oxygen isotope fractionations in zircon. *Geochim. Cosmochim. Acta* 67:3257–3266.
- Veksler, I. V.; Dorfman, A. M.; Borisov, A. A.; Wirth, R.; and Dingwell, D. B. 2007. Liquid immiscibility and the evolution of basaltic magma. *J. Petrol.* 48:2187–2210.
- Wager, L. R., and Brown, G. M. 1967. *Layered igneous rocks*. San Francisco, W. H. Freeman, 588 p.
- Wager, L. R., and Deer, W. A. 1939. Geological investigations in East Greenland. III. The petrology of the Skaergaard intrusion, Kangerdlugssuaq, East Greenland. *Medd. Grøn.* 105:352.
- Watson, E. B.; Wark, D. A.; and Thomas, J. B. 2006. Crystallization thermometers for zircon and rutile. *Contrib. Mineral. Petrol.* 151:413–433.
- Xirouchakis, D.; Lindsley, D. H.; and Frost, B. R. 2001. Assemblages with titanite (CaTiOSiO₄), Ca-Mg-Fe olivine and pyroxenes, Fe-Mg-Ti oxides, and quartz. II. Application. *Am. Mineral.* 86:254–264.